J Supercond Nov Magn (2017) 30:1359–1366
DOI 10.1007/s10948-016-3645-5

ORIGINAL PAPER

Engineering of Giant Magnetoimpedance Effect of Amorphous and Nanocrystalline Microwires

A. Zhukov[1,2,3] · M. Ipatov[1,2] · A. Talaat[1,2] · J. M. Blanco[2] · M. Churyukanova[4] · A. Granovsky[5] · V. Zhukova[1,2]

Received: 11 May 2016 / Accepted: 19 July 2016 / Published online: 28 July 2016

Abstract We present an overview of the factors affecting soft magnetic properties and giant magnetoimpedance (GMI) effect of thin amorphous wires. Low coercivity and high GMI effect have been observed in as-prepared Co-rich microwires. We showed that the magnetoelastic anisotropy is one of the most important parameters that determines the magnetic softness and GMI effect of glass-coated microwires, and annealing can be very effective for manipulation of the magnetic properties of amorphous ferromagnetic glass-coated microwires. After annealing of Co-rich microwires, we can observe the transformation of inclined hysteresis loops to rectangle and coexistence of fast magnetization switching and GMI effect in the same sample. We demonstrated that the switching field value of microwires can be tailored by annealing in the range from 4 to 200 A/m. On the other hand in Fe-rich FeCuNbSiB microwires after appropriate annealing, we observed considerable magnetic softening and GMI effect enhancement.

Keywords Magnetic microwires · Giant magnetoimpedance · Magnetoelastic anisotropy · Magnetostriction · Nanocrystals

1 Introduction

Recent advances in the technologies involving magnetic materials require the development of novel functional magnetic materials with improved magnetic and magnetotransport properties. In addition, the tendency on miniaturization of the modern magnetic sensors and devices stimulates the development of such magnetic materials with reduced dimensionality. Certain progress has been recently achieved in thin soft magnetic wires and, in particular, glass-coated microwires thanks to outstanding magnetic properties and their potential applications in various industrial sectors such as magnetic sensors, microelectronics, and security [1–3]. These microwires consist of a metallic nucleus with a typical diameter from 1 up to 30 μm and glass coating sheath with a thickness from 1 to 10 μm and can be prepared by the modified Taylor-Ulitovsky technique based on the rapid quenching from the molten metal [1–4]. The main advantage of these microwire is related to the small dimensions, circular symmetry, high efficiency (possibility to produce continues microwires up to few kilometers only from 1 g of master alloy), and simple and cheap fabrication process. Moreover, the glass coating itself provides an electrical insulation and enhances biocompatibility.

The main interest in amorphous soft magnetic materials is related to their liquid-like structure characterized by the

✉ A. Zhukov
arkadi.joukov@ehu.es

1 Departamento de Física Mater, Basque Country University, San Sebastián 20018, Spain

2 Departamento de Física Aplicada, EUPDS, Basque Country University, San Sebastián 20018, Spain

3 IKERBASQUE, Basque Foundation for Science, Bilbao 48011, Spain

4 National University of Science and Technology "MISiS", Moscow 119049, Russia

5 Moscow State "Lomonosov" University, Moscow, Russia

absence of long-range ordering. In other words, the absence of magnetocrystalline anisotropy is the main reason of extremely soft magnetic properties exhibited by amorphous magnetic materials [1, 4]. Therefore, their magnetic properties are determined mainly by magnetoelastic anisotropy. This magnetoelastic anisotropy, K_{me}, is regulated by the internal stresses and the magnetostriction coefficient, which is given by the following equation [2]:

$$K_{me} = 3/2\lambda_s\sigma_i\lambda \quad (1)$$

where λ_s is the saturation magnetostriction and σ_i is the internal stress induced by the glass coating layer during the fabrication technique of glass-coated microwires.

The difference in the thermal expansion coefficients between the glass sheath and the ferromagnetic nucleus introduces considerable internal stresses inside the metallic nucleus, σ_i [5–7]. The strength of the internal stresses depends on the ρ ratio between the metallic nucleus diameter, d, and total microwire diameter, D ($\rho = d/D$) [5–7], increasing with the decrease of the ρ ratio, i.e., with the increase of the relative volume of the glass coating, while the magnetostriction coefficient mostly depends on the chemical composition and vanishes in amorphous Fe-Co-based alloys with Co/Fe = 70/5 [4, 5].

On the other hand, the so-called "nanocrystalline materials," that is, two-phase systems consisting of nanocrystalline grains randomly distributed in a soft magnetic amorphous phase, attracted great attention owing to excellent magnetic softness and high saturation magnetization [8–10]. After crystallization, such material consists of small (around 10 nm grain size) nanocrystallites embedded in the residual amorphous matrix. Aforementioned magnetic softness is thought to be originated from the vanished magnetocrystalline anisotropy and the very low magnetostriction value when the grain size approaches 10 nm [9, 10].

One of the most promising and relevant applications of soft magnetic amorphous materials is related to the so-called "giant magnetoimpedance effect" (GMI). This GMI effect defined as the large change of the electrical impedance of a magnetic conductor when it is subjected to an axial dc magnetic field, H [11, 12]. It has been recognized that the large sensitivity of the total impedance of a soft magnetic conductor at low magnetic fields and high frequencies of the driven ac current originates from the dependence of the transverse magnetic permeability upon the dc magnetic field and skin effect. Large GMI effect (up to 600 %) has been reported for Co-based amorphous glass-coated microwires with nearly zero magnetostriction sign [13, 14]. This extremely high magnetic field sensitivity allows using of soft magnetic materials for creation of sensitive and cheap magnetic sensors and magnetometers [15–18].

Additionally, the GMI effect exhibited by amorphous wires is quite sensitive to external stimuli, such as stress, temperature that enables them for the use in detection of stresses, and/or temperature variation [19–21].

Although initially GMI effect has been mostly reported in amorphous microwires [13–15, 18], recently, we observed in Finemet-type glass-coated microwires [22, 23]. It is worth mentioning that, usually, the GMI effect of Fe-rich amorphous materials is rather low due to low magnetic permeability [23]. Therefore, magnetic softening obtained after the nanocrystallization is essential for the optimization of the GMI effect in nanocrystalline materials. Meanwhile, the substitution of Co-rich amorphous microwires by less-expensive Fe-rich microwires can be essentially promising from industrial application's point of view. Therefore, optimizing high GMI effect in Fe-rich glass-coated microwires is nowadays one of the relevant topics of research.

The aim of this paper is to illustrate experimentally the fundamental features in order to optimize high GMI effect in Co-rich amorphous and Finemet glass-coated microwires fabricated by the Taylor-Ulitovsky technique.

2 Experimental Details

We studied glass-coated $Co_{69.2}Fe_{4.1}B_{11.8}Si_{13.8}C_{1.1}$ ($d = 25.6$ μm, $D = 30.2$ μm, $\rho = 0.84$) and $Co_{50.69}Fe_{8.13}Ni_{17.55}B_{13.29}Si_{10.34}$ ($d = 12.8$ μm, $D = 15.8$ μm, $\rho = 0.81$) microwires and $Fe_{70.8}Cu_1Nb_{3.1}Si_{14.5}B_{10.6}$ ($d = 10.7$ μm, $D = 16.4$ μm, $\rho = 0.6$) prepared by the Taylor-Ulitovsky technique (also called in some publications as the drawing and quenching technique) described elsewhere [1–4]. This method is essentially based on the direct casting from the melt and consists of a simultaneous drawing of the composite microwire (metallic nucleus inside the glass capillary) through the quenching liquid (water or oil) jet onto rotating bobbins.

Hysteresis loops of as-prepared and annealed microwires were measured by the induction method [3]. We represent the normalized magnetization, M/M_0, versus magnetic field, H, where M is the magnetic moment at the given magnetic field and M_0 is the magnetic moment of the sample at the maximum magnetic field amplitude, H_0.

We measured the magnetic field dependences of impedance, Z, and GMI ratio, $\Delta Z/Z$. We used the specially designed microstrip sample holder placed inside a sufficiently long solenoid that creates a homogeneous magnetic field, H. One wire end was connected to the inner conductor of a coaxial line through a matched microstrip line, while the other was connected to the ground plane. This sample holder allows measuring the samples of 6 mm in length. This sample length is sufficiently long, allowing neglecting the effect of the demagnetizing factor [3, 8]. We determined the impedance Z using the vector network analyzer from reflection coefficient S_{11}. The employed method allowed

extending the frequency range up to gigahertz range [8]. The magnetoimpedance ratio, $\Delta Z/Z$, has been defined as

$$\Delta Z/Z = [Z(H) - Z(H_{max})] \cdot 100/Z(H_{max}) \quad (2)$$

where an axial dc field with maximum value, H_{max}, up to 20 kA/m was supplied by magnetization coils.

The microwires have been annealed with and without stress in conventional furnace at temperatures, T_{ann}, of 200–300 °C for the duration, t_{ann}, from 5 to 60 min. After annealing, the magnetic properties of microwires were studied again.

In order to obtain the nanocrystalline structure, we have selected $Fe_{70.8}Cu_1Nb_{3.1}Si_{14.5}B_{10.6}$ that can be considered as a typical FeSiB metallic glass composition with small additions of Cu and Nb [7–9]. For this alloy, annealing was carried out in temperatures, T_{ann}, of 400–650 °C for 1 h. Structure and phase composition have been checked using a Bruker (D8 Advance) X-ray diffractometer with Cu Kα ($\lambda = 1.54$ Å) radiation.

The magnetostriction coefficient of studied microwires has been measured using a SAMR method described elsewhere and recently successfully employed for the case of magnetic microwires [24, 25].

Essentially in this method, the sample is saturated by an axial magnetic field, H, while applying simultaneously a small ac transverse field, H_y, created by an ac electric current flowing along the sample. The combination of these fields leads to a reversible rotation of the magnetization within a small angle, θ, out of the axial direction. The induction voltage, $V(2\omega)$, due to the magnetization rotation is detected by a pickup coil wound around the microwire. The magnetostriction constant is determined from the measurement of the dependence on axial magnetic field, H, versus that on applied stress σ at a fixed value of induction voltage, $V(2\omega)$. The $\mu_0 M_s$ values of the investigated microwires were obtained from room-temperature measurements of the magnetization curves at high magnetic field. The ac current value, $i \sim$, flowing through the wire is selected to avoid possible Joule heating of the sample: the current amplitude does not exceed 10–30 mA.

3 Experimental Results and Discussion

3.1 Tailoring of Magnetic Properties and GMI Effect in Co-Rich Amorphous Microwires

As can be seen from Fig. 1a, b, the as-prepared $Co_{69.2}Fe_{4.1}B_{11.8}Si_{13.8}C_{1.1}$ and $Co_{50.69}Fe_{8.13}Ni_{17.55}B_{13.29}Si_{10.34}$ microwires present quasi-linear hysteresis loops and amorphous structure (consisted of a diffuse halo without an observation of any crystalline peak) as shown in XRD in Fig. 1c. A coercive field of both samples is about 4 A/m that

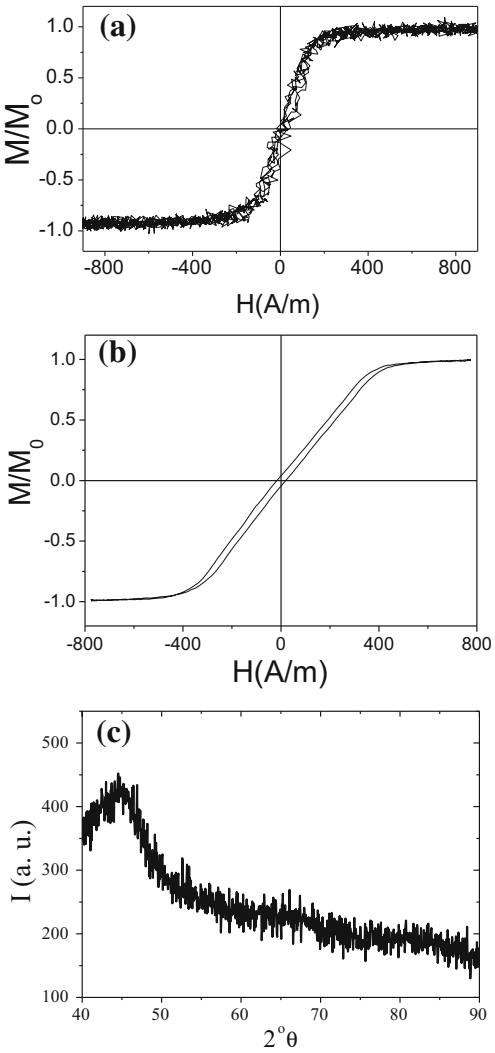

Fig. 1 Hysteresis loop of the as-prepared $Co_{69.2}Fe_{4.1}B_{11.8}Si_{13.8}C_{1.1}$ (**a**) and $Co_{50.69}Fe_{8.13}Ni_{17.55}B_{13.29}Si_{10.34}$ (**b**) microwires and XRD patterns (**c**) for the as-prepared $Co_{69.2}Fe_{4.1}B_{11.8}Si_{13.8}C_{1.1}$ glass-coated microwires

is typical for amorphous Co-based glass-coated microwires with low negative magnetostriction constant. The internal stresses of as-prepared microwires give rise to an easy magnetization direction perpendicular to the wire axis, leading to an alignment of the magnetic moments in the direction which is perpendicular (circumferential) to the wire axis. As a consequence, mostly the magnetization rotation processes with low coercivity are observed when an axial magnetic field is applied. On the other hand, annealing even for quite short time and at low temperature leads to significant changes of the magnetic properties of both studied Co-rich microwires (Figs. 2a–d and 3a–c). By increasing the annealing time and temperature, the hysteresis loop becomes more rectangular: remanent magnetization rises with an increase in T_{ann}, although coercivity, H_c, remains almost the same for all annealing conditions.

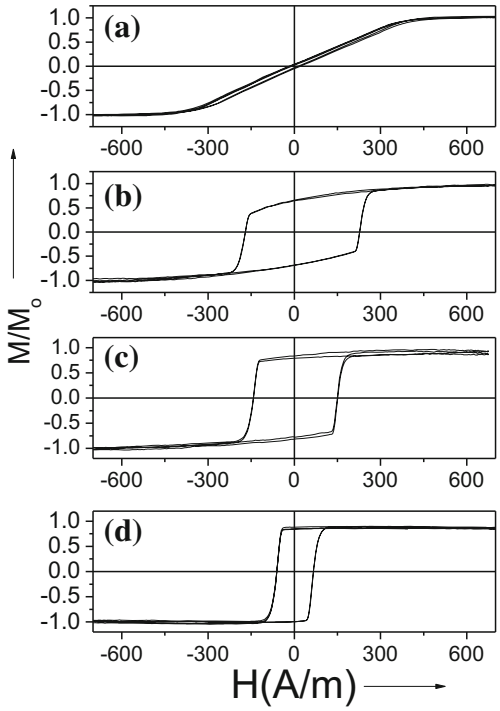

Fig. 2 Hysteresis loops of the as-prepared (**a**) and annealed for 5 min at 200 °C (**b**), 250 °C (**c**), and 300 °C (**d**) $Co_{50.69}Fe_{8.13}Ni_{17.55}B_{13.29}Si_{10.34}$ microwires

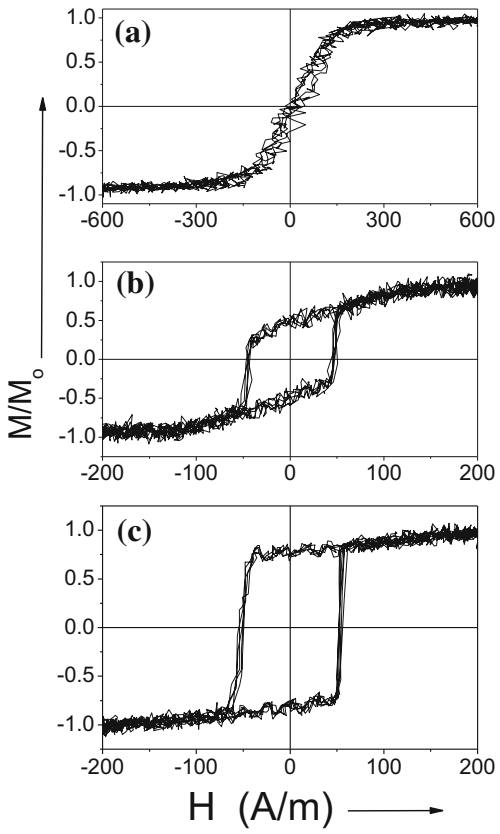

Fig. 3 Hysteresis loops of the as-prepared (**a**) and annealed for 5 min at 200 °C (**b**) and 300 °C (**c**) $Co_{69.2}Fe_{4.1}B_{11.8}Si_{13.8}C_{1.1}$ microwires

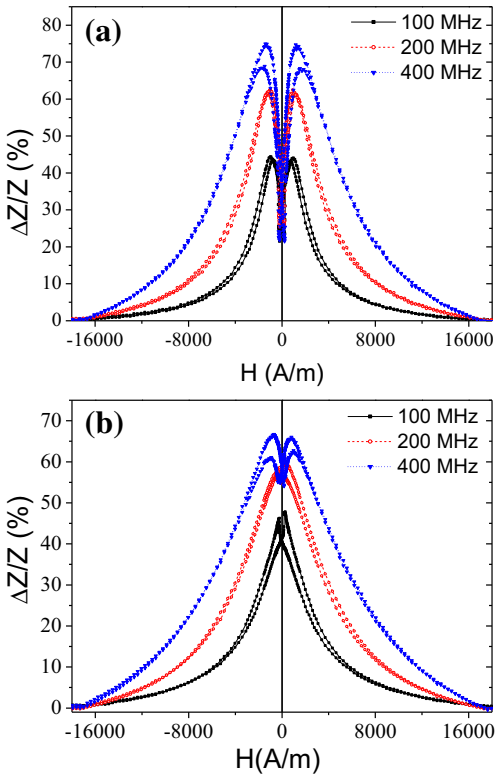

Fig. 4 $\Delta Z/Z(H)$ dependences of the as-prepared (**a**) and annealed at 200 °C for 5 min (**b**) $Co_{50.69}Fe_{8.13}Ni_{17.55}B_{13.29}Si_{10.34}$ microwires measured at different frequencies

In spite of considerable magnetic hardening (the most remarkable increase of coercivity from 4 to 200 A/m for the $Co_{50.69}Fe_{8.13}Ni_{17.55}B_{13.29}Si_{10.34}$ sample), both as-prepared and annealed microwires at different annealing conditions present a considerable GMI effect as shown in Figs. 4 and 5.

The main difference of the observed $\Delta Z/Z(H)$ dependences for as-prepared and annealed samples is the value of the magnetic field, H_m, at which $\Delta Z/Z$ maximum takes place: for annealed samples, H_m values are much lower than those for as-prepared samples for all measured frequencies. Additionally, we observed an increase of the GMI effect with an increase of the frequency, f, for as-prepared and annealed samples at temperatures (T_{ann}) up to 250 °C (see Figs. 4 and 5). But for the sample annealed at $T_{ann} = 300$ °C, $\Delta Z/Z$ measured at $f = 400$ MHz is lower than that for $f = 200$ MHz (see Fig. 5b).

Figure 6a shows the hysteresis loops of $Co_{69.2}Fe_{4.1}B_{11.8}Si_{13.8}C_{1.1}$ glass-coated microwires annealed at $T_{ann} = 300$ °C for 45 min without stress and under tensile stress of about 80 MPa.

As can be assumed, stress-annealed microwires exhibit lower coercivity as compared to conventional annealed samples (Fig. 6a). Herein, we must consider the back stresses arising during the stress annealing as previously reported for Fe- and Co-based amorphous microwires [26, 27]. Such

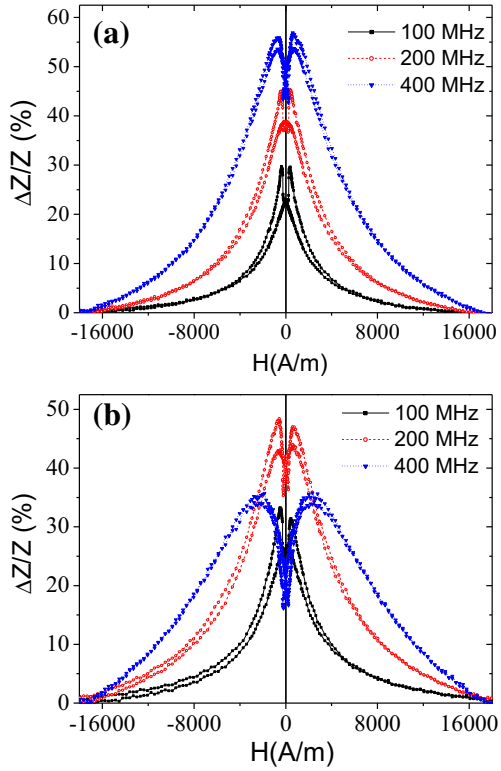

Fig. 5 $\Delta Z/Z(H)$ dependences of the annealed $Co_{50.69}Fe_{8.13}Ni_{17.55}B_{13.29}Si_{10.34}$ microwires for 60 min at 250 °C (**a**) and 300 °C (**b**) that were measured at different frequencies

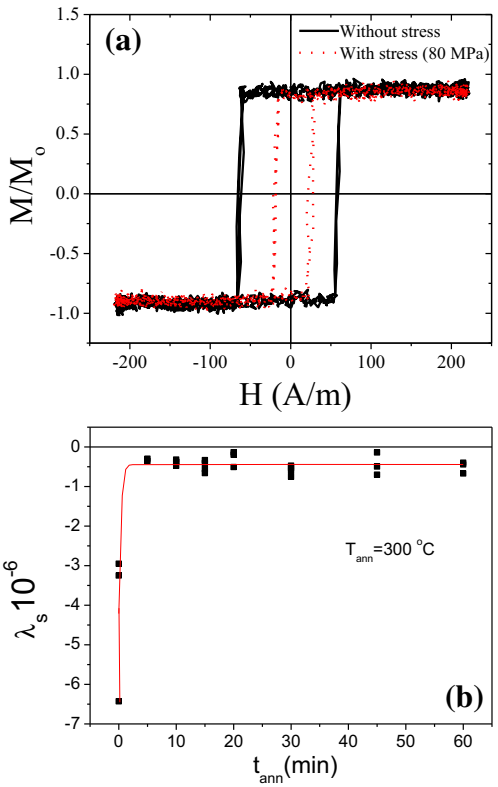

Fig. 6 Hysteresis loops of the annealed $Co_{69.2}Fe_{4.1}B_{11.8}Si_{13.8}C_{1.1}$ glass-coated microwires at $T_{ann} = 300$ °C for 45 min without stress and under tensile stress of about 80 MPa (**a**), and magnetostriction dependence on annealing time for stress-annealed $Co_{69.2}Fe_{4.1}B_{11.8}Si_{13.8}C_{1.1}$ microwire samples at $T_{ann} = 300$ °C/80 MPa (**b**)

back stresses can result in a decrease of the magnetostriction constant according the following equation:

$$\lambda_s(\sigma) = \lambda_s(0) - B\sigma \tag{3}$$

where $\lambda_s(\sigma)$ is the magnetostriction constant under stress,$\lambda_s(0)$ is the zero-stress magnetostriction constant, is the positive coefficient of order 10^{-10} MPa, and σ is the stresses. Furthermore, as experimentally shown in Fig. 6b, the magnetostriction considerably changes after annealing to nearly zero for annealed $Co_{69.2}Fe_{4.1}B_{11.8}Si_{13.8}C_{1.1}$ microwire samples after annealing at $t_{ann} \geq 5$ min.

In addition, if the magnetostriction coefficient is low and negative, we must consider two opposite consequences of the internal stresses. The first contribution is an increase of the total magnetoelastic energy given by (1). The second one must be related to the stress dependence (either applied or internal stresses: $\sigma_{total} = \sigma_{applied} + \sigma_{internal}$) on magnetostriction coefficient described by (3), which is quite relevant for the case of low magnetostriction constant, $\lambda_{s,0}$. Accordingly, the magnetostriction constant under stress, $\lambda_{s,\sigma}$, must be decreased. Based on the dependencies observed in Figs. 2 and 3, the increase of coercivity and rectangular character of hysteresis loops after annealing must be attributed to the stress relaxation and corresponding magnetostriction changes. We can also assume that the outer domain shell of the annealed Co-rich microwire that exhibits both a rectangular hysteresis loop and a GMI effect presents high circumferential magnetic permeability. This assumption is deduced by observing the much higher GMI ratio of Co-rich microwires that exhibit a rectangular hysteresis loop after annealing than those of the Fe-rich amorphous microwires also exhibiting similar bulk hysteresis loop characteristics but much lower GMI effect (usually about 1–5 %) [23].

We have also aimed to compare between either GMI responses in as-prepared stress and conventional annealed $Co_{69.2}Fe_{4.1}B_{11.8}Si_{13.8}C_{1.1}$ microwire samples at the same annealing conditions as shown in Fig. 7.

As can be observed in Fig. 7, GMI responses likely increase for stress-annealed microwire samples: $\Delta Z/Z_{max}$ (measured at $f = 200$ MHz) increases from 160 % of conventional annealed microwires up to $\approx$ 325 % for the case of stress annealing. This difference must be attributed to the lower coercivity of stress-annealed microwires (similar to those observed in Fig. 6a). Consequently, stress annealing is the perspective method for optimization of the GMI effect in Co-rich samples.

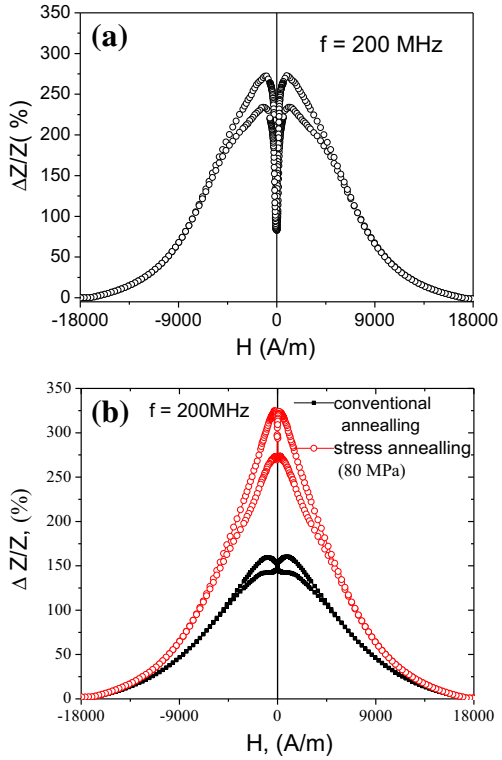

Fig. 7 $\Delta Z/Z(H)$ dependencies of the as-prepared (**a**) conventional and stress-annealed (at $T_{ann} = 300\,^{\circ}C$ for $t_{ann} = 5$ min) (**b**) $Co_{69.2}Fe_{4.1}B_{11.8}Si_{13.8}C_{1.1}$ glass-coated microwires

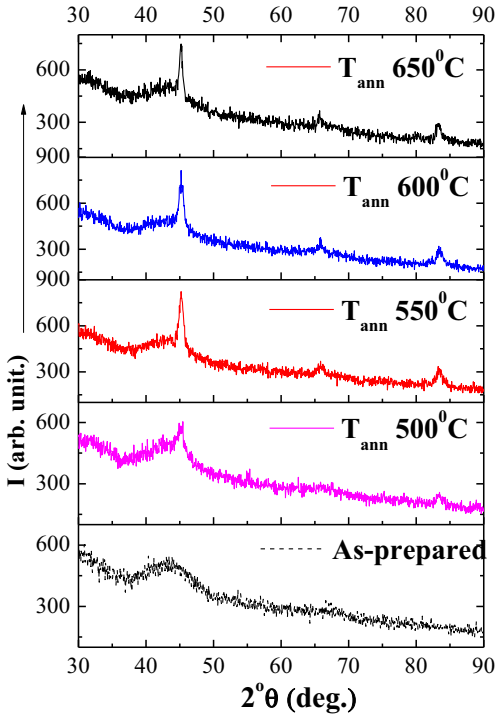

Fig. 8 XRD patterns of the as-prepared and annealed $Fe_{70.8}Cu_1Nb_{3.1}Si_{14.5}B_{10.6}$ glass-coated microwires at different temperatures for 1 h

3.2 Tailoring of GMI Effect in Nanocrystalline Fe-Rich Microwires

Usually, the basic method to obtain a nanocrystalline structure from the amorphous state is to control the crystallization kinetics by optimizing the heat treatment conditions (annealing temperature, annealing time, heating rate, etc.). The evolution of structural and magnetic properties of the $Fe_{70.8}Cu_1Nb_{3.1}Si_{14.5}B_{10.6}$ microwire has been studied in different annealing temperatures in the range between 400 and 650 °C for 1 h in order to investigate the devitrification process (Fig. 8). Starting from 550 to 650 °C, a main crystalline peak is appearing in the range between 42° and 45° which corresponds to the existence of α-Fe(Si) BCC crystal structure [7–9], and another two weak peaks appear in the range between 65° and 85°.

The grain size has been estimated based on the Scherrer equation as we previously reported [28]. From this analysis, we can underline that the grain size of studied microwires increases from 17 to 22 nm upon increasing the annealing temperature from 550 to 650 °C, respectively.

Finally, the presence of the remaining amorphous phase is not required to reduce the net magnetocrystalline anisotropy, but such existence of these two phases gives a good balance of positive and negative magnetostriction (λ_s), resulting finally in a very low net magnetostriction, according to the following equation:

$$\lambda_{s,eff} = V_{cr}\lambda_{s,cr} + (1 - V_{cr})\lambda_{s,am} \quad (4)$$

where $\lambda_{s,eff}$ is the saturation magnetostriction coefficient and V_{cr} is the crystalline volume fraction.

Consequently, the enhanced soft magnetic properties of these kinds of material can be achieved. As can be observed from Fig. 9, a considerable magnetic softening is observed after sample annealing. The dependence of coercivity, H_c, on annealing temperature is shown in Fig. 9.

Generally, a decrease of coercivity has been observed at annealing temperatures below 600 °C as displayed in Fig. 9.

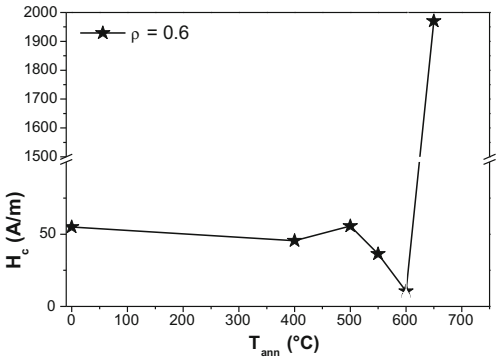

Fig. 9 Coercivity dependence on the annealing temperature measured in the $Fe_{70.8}Cu_1Nb_{3.1}Si_{14.5}B_{10.6}$ microwire with $\rho = 0.6$

Magnetic softening (the optimum softest behavior) with a quite low value of coercivity is obtained in the samples treated at T_{ann} ≈500–600 °C which is ascribed to the fact that the first crystallization process has been developed, leading to fine nanocrystals α-Fe(Si) of grain size around 10–20 nm, and it has been widely reported for Finemet ribbons (see, for example, ref. [9]). An abrupt increase of the coercivity is observed in the samples treated at temperature above 600 °C, indicating that the beginning of such increase should be connected to the precipitation of iron borides (with grain size larger than 50 nm) and deterioration of the magnetic softness.

Considering the magnetic softening observed after devitrification of the studied sample, we measured the GMI effect. Figure 10 displays the $\Delta Z/Z(H)$ dependence of the as-prepared samples and annealed $Fe_{70.8}Cu_1Nb_{3.1}Si_{14.5}B_{10.6}$ sample. As was expected, the microwire samples with amorphous structure exhibit rather poor GMI responses (≈ 7 % for $Fe_{70.8}Cu_1Nb_{3.1}Si_{14.5}B_{10.6}$) typical for Fe-based glass-coated microwires with highly positive magnetostriction. The significant influence of the nanocrystallization on optimizing GMI effect is visible in Fig. 10b. Interestingly, the GMI responses show a remarkable improvement of annealed $Fe_{70.8}Cu_1Nb_{3.1}Si_{14.5}B_{10.6}$ microwire samples at $T_{ann} = 550$ °C, with GMI effect being considerably enhanced from 11 to 130 % for $f = 600$ MHz (Fig. 10). These observed experimental results are, indeed, of practical interest for GMI-related applications, particularly in tunable metamaterial applications recently proposed by various authors [29, 30].

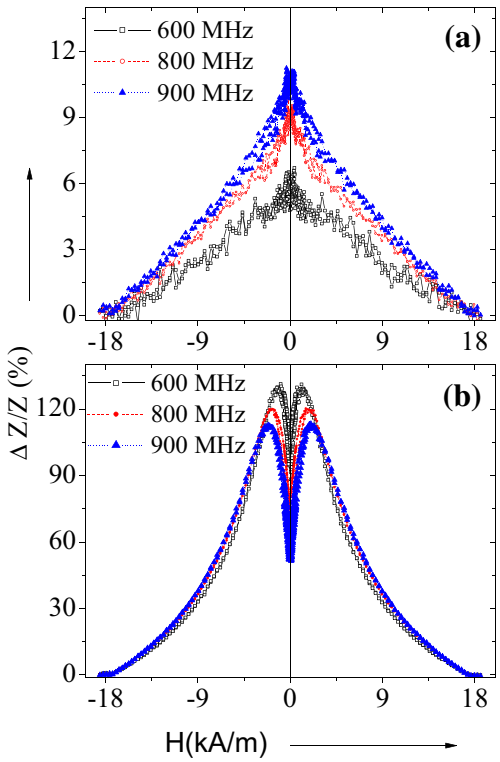

Fig. 10 $\Delta Z/Z(H)$ dependences of the as-prepared (**a**) and annealed at $T_{ann} = 550$ °C (**b**) $Fe_{70.8}Cu_1Nb_{3.1}Si_{14.5}B_{10.6}$ microwires ($\rho = 0.6$) measured at different frequencies

4 Conclusions

We investigated the possibility to control the magnetic properties of amorphous ferromagnetic microwires by annealing. We demonstrated that annealing conditions drastically affect the magnetic properties. We observed that annealing of amorphous Co-rich microwire considerably affects its hysteresis loop and GMI effect. The observed dependences of these characteristics are attributed to stress relaxation and changes in the magnetostriction after sample annealing. A drastic change of coercivity after annealing in the range between 400 and 650 °C measured in nanocrystalline FINEMET glass-coated microwires is explained in terms of the devitrification process caused by thermal annealing. Enhancement of GMI has been observed upon annealing, which affirm the optimum magnetic softness of the FINEMET glass-coated microwires. We believe that FINEMET-type glass-coated microwires with higher saturation magnetization are good candidates for the GMI sensor and metacomposite applications.

Acknowledgments This work was supported by the Spanish MINECO under MAT2013-47231-C2-1-P and by the Russian Science Foundation under the 16-19-10490 grant. The technical and human support provided by SGIker (UPV/EHU, MICINN, GV/EJ, ERDF, and ESF) is gratefully acknowledged. VZ and AZ wish to acknowledge the support of the Basque Government under the Program of Mobility of the Researchers of the Basque Government (grants MV-2016-1-0025 and MV-2016-1-0018, respectively).

References

1. Vazquez, M., Chiriac, H., Zhukov, A., Panina, L., Uchiyama, T.: Phys. Status Solidi A **208**, 493–501 (2011)
2. Phan, M.H., Peng, H.X.: Prog. Mater. Sci. **53**, 323–420 (2008)
3. Zhukov, A., Vázquez, M., Velázquez, J., Hernando, A., Larin, V.: J. Magn. Magn. Mat. **170**, 323–330 (1997)
4. Ekstrom, P.A., Zhukov, A.: J. Phys. D: Appl. Phys. **43**, 205001 (2010)
5. Chiriac, H., Ovari, T.A., Zhukov, A.: J. Magn. Magn. Mater. **254–255**, 469–471 (2003)
6. Zhukov, A., Blanco, J.M., Ipatov, M., Chizhik, A., Zhukova, V.: Nanoscale Res. Lett. **7**, 223 (2012)
7. Antonov, A.S., Borisov, V.T., Borisov, O.V., Prokoshin, A.F., Usov, N.A.: J. Phys. D: Appl. Phys. **33**, 1161–1168 (2000)
8. Yoshizawa, Y., Oguma, S., Yamauchi, K.: J. Appl. Phys. **64**, 6044–6046 (1988)
9. Herzer, G.: IEEE Trans. Magn **26**, 1397–1402 (1990)
10. Herzer, G.: J. Magn. Magn Mater. **157/158**, 133–136 (1996)
11. Panina, L.V., Mohri, K.: Appl. Phys. Lett. **65**, 1189–1191 (1994)

12. Beach, R., Berkowitz, A.: Appl. Phys. Lett. **64**, 3652–2654 (1994)
13. Zhukova, V., Chizhik, A., Zhukov, A., Torcunov, A., Larin, V., Gonzalez, J.: IEEE Trans. Magn. **38**, 3090–3092 (2002)
14. Pirota, K.R., Kraus, L., Chiriac, H., Knobel, M.: J. Magn. Magn Mater. **221**, L243–L247 (2000)
15. Honkura, Y.: J. Magn. Magn. Mater. **249**, 375–377 (2002)
16. Mohri, K., Uchiyama, T., Shen, L.P., Cai, C.M., Panina, L.V.: J. Magn. Magn. Mater. **249**, 351–356 (2002)
17. Dufay, B., Saez, S., Dolabdjian, C.P., Yelon, A., Ménard, D.: IEEE Sensors J. **13**(1), 379–388 (2013)
18. Gudoshnikov, S., Usov, N., Nozdrin, A., Ipatov, M., Zhukov, A., Zhukova, V.: Phys. Status Solidi A **211**(5), 980–985 (2014)
19. Blanco, J.M., Zhukov, A., Gonzalez, J.: J. Magn. Magn. Mat. **196-197**, 377–379 (1999)
20. Blanco, J.M., Zhukov, A., Gonzalez, J.: J. Phys. D:Appl. Phys. **32**, 3140–3145 (1999)
21. Zhukova, V., Blanco, J.M., Ipatov, M., Zhukov, A., Garca, C., Gonzalez, J., Varga, R., Torcunov, A.: Sensors Actuators B **126**, 318–323 (2007)
22. Zhukov, A., Talaat, A., Ipatov, M., Zhukova, V.: IEEE Magn. Lett. **6**, 2500104 (2015)
23. Zhukov, A., Talaat, A., Ipatov, M., Blanco, J.M., Gonzalez-Legarreta, L., Hernando, B., Zhukova, V.: IEEE Trans. Magn. **50**(6), 2501905 (2014)
24. Narita, K., Yamasaki, J., Fukunaga, H.: IEEE Trans. Magn., Magn. **16**, 435–439 (1980)
25. Zhukov, A., Churyukanova, M., Kaloshkin, S., Sudarchikova, V., Gudoshnikov, S., Ipatov, M., Talaat, A., Blanco, J.M., Zhukova, V.: J. Electr. Mater. **45**(1), 226–234 (2016)
26. Zhukov, A., Chichay, K., Talaat, A., Rodionova, V., Blanco, J.M., Ipatov, M., Zhukova, V.: J. Magn. Magn. Mater. **383**, 232–236 (2015)
27. Zhukov, A., Talaat, A., Ipatov, M., Blanco, J.M., Zhukova, V.: J. Alloys Compounds **615**, 610–615 (2014)
28. Talaat, A., del Val, J.J., Zhukova, V., Ipatov, M., Klein, P., Varga, R., Gonzalez, J., Churyukanova, M., Zhukov, A.: J. Magn. Magn. Mat. **406**, 15–21 (2016)
29. Qin, F.X., Peng, H.X., Phan, M.H., Panina, L.V., Ipatov, M., Zhukov, A.: Sensors Actuators A **178**, 118–125 (2012)
30. Ipatov, M., Zhukova, V., Zhukov, A., Panina, L.V.: Advances in Science and Technology **75**, 224–229 (2010)